Roles of Cytoplasmic Arginine and Threonine in Chloride Transport by the Bacteriorhodopsin Mutant D85T

Stefan Paula, Jörg Tittor, and Dieter Oesterhelt
Department of Membrane Biochemistry, Max Planck Institute of Biochemistry, 82152 Martinsried, Germany

ABSTRACT In the light-driven anion pump halorhodopsin (HR), the residues arginine 200 and threonine 203 are involved in anion release at the cytoplasmic side of the membrane. Because of large sequence homology and great structural similarities between HR and bacteriorhodopsin (BR), it has been suggested that anion translocation by HR and by the chloride-pumping BR mutant BR-D85T occurs by the same mechanism. Consequently, the functions of the R200/T203 pair in HR should be the same as those of the corresponding pair in BR-D85T (R175/T178). We have put this hypothesis to a test by creating two mutants of BR-D85T in which R175 and T178 were replaced by glutamine and valine, respectively. Chloride transport activities were essentially the same for all three mutants, whereas chloride binding and the kinetics of parts of the photocycle were markedly affected by the replacement of T178. In contrast, the consequences of mutating R175 proved to be less significant. These findings are consistent with evidence obtained on HR and therefore support the idea that the respective mechanistic roles of the cytoplasmic arginine/threonine pairs in HR and BR-D85T are equal.

INTRODUCTION

The only currently known light-driven anion pumps are halorhodopsin (HR) (Lanyi, 1990; Oesterhelt, 1995) and certain mutants of bacteriorhodopsin (BR) in which aspartate 85 is replaced by a serine or threonine residue (Tittor et al., 1994, 1997; Sasaki et al., 1995). Both proteins use light energy to transport chloride ions against an unfavorable electrochemical gradient into the cells of halobacteria. Formally, the sequence of events leading to ion translocation in retinal proteins can be described by the so-called IST model (Haupts et al., 1997; Oesterhelt, 1998), which classifies the individual catalytic steps as isomerization (I), transfer (T), and accessibility switch (S) processes. In HR, for example, photoisomerization of the retinal (I*) induces the movement of an anion from the extracellular binding site past the protonated Schiff base (T). This event is followed by an accessibility switch (S) from the extracellular to the cytoplasmic site and the release of the ion into the cytoplasm (T). Thermal re-isomerization (I), a second accessibility switch (S), and the re-uptake of a chloride ion at the binding site complete the catalytic cycle, which can be summarized as I*TSTIS. Despite the availability of such schemes for HR and BR-D85T (Oesterhelt, 1998), the atomic details of the translocation mechanism are still not known.

Significant progress toward understanding the mechanism of anion translocation was made recently by solving the structure of HR by x-ray diffraction after crystallizing the protein in the cubic lipidic phase (Kolbe et al., 2000). Nevertheless, this study provides information only on the unphotolyzed state of the protein whereas the structures of the intermediate states, which are necessary for a complete picture, are yet unknown. So far, time-resolved visible and infrared spectroscopy (Tittor et al., 1987; Zimányi and Lanyi, 1989a; Váró et al., 1995a,b,c; Ames et al., 1992; Dioumaev and Braiman, 1997), photoelectric measurements (Kalaidzidis et al. 1998; Ludmann et al., 2000), site-directed mutagenesis (Rüdiger et al., 1995; Rüdiger and Oesterhelt, 1997), and crytotrapping studies (Zimányi et al. 1989; Zimányi and Lanyi, 1989b) have been the methods of choice to gather information on the HR photocycle and its intermediates that are essential for anion transport. Even less mechanistic information is available on the mutants BR-D85T and BR-D85S. No three-dimensional structure has been determined to date, and most of the experimental evidence stems from electrical measurements (Tittor et al., 1994; Kalaidzidis and Kaulen, 1997) and time-resolved optical spectroscopy (Sasaki et al., 1995; Brown et al., 1996; Tittor et al., 1997).

Mutagenesis studies of HR identified the functions of two symmetric, highly conserved arginine/threonine pairs in the transmembrane region of the protein (Rüdiger and Oesterhelt, 1997). Whereas the extracellular pair R108/T111 is primarily responsible for anion binding in the unphotolyzed state, the cytoplamsic pair R200/T203 displays a catalytic function during anion release into the cytoplasm. It was demonstrated that mutations in the positions of the cytoplasmic pair diminished chloride transport activity by reducing the photocycling rate of the protein. Because the effects were most prominent in the case of T203 mutations, the authors postulated that the threonine facilitates anion permeation from the Schiff base to the cytoplasm via direct interactions with the transported anion during its release through the cytoplasmic part of the translocation pathway. The three-dimensional structure of HR supports this assignment by locating a water molecule in close proximity to T203 (Kolbe et al., 2000). Water molecules along the ion translocation pathway in proteins are believed to be crucial

Received for publication 28 September 2000 and in final form 31 January 2001.

Address reprint requests to Dr. Jörg Tittor. E-mail: tittor@biochem.mpg.de.

0006-3495/01/05/2386/10 $2.00

because they can help solvate and energetically stabilize the transported ion as it enters predominantly hydrophobic parts of the protein. Mutation of R200 also reduced the photocycling rate, but to a lesser extent. This led to the conclusion that R200 does not interact directly with the transported halide ion and that its replacement might induce a small disarrangement of the local protein structure with a rather moderate effect on ion release.

Sasaki et al. (1995) and Tittor et al. (1997) showed that a single mutation (D85T) converts the proton pump BR into an anion pump which, like HR, transports chloride ions from the extracellular to the cytoplasmic compartment of the cell. This remarkable finding along with prominent similarities both in sequence (Oesterhelt, 1995; Ihara et al., 1999) and in structure (Luecke et al., 1999a; Kolbe et al., 2000) strongly suggests that the mechanism of ion translocation by the two systems is similar or even identical. If correct, this implies that the functions of R200 and T203 in HR are assumed by the conserved residues R175 and T178 in BR-D85T. As a consequence, the effects of their mutation should match those seen in HR. In particular, one would expect to see changes in those parts of the photocycle that are associated with anion release.

Briefly, the first intermediate in the photocycle of both HR (HR_{600}) (Tittor et al., 1987; Váró et al., 1995c) and of BR-D85T (Sasaki et al., 1995; Tittor et al., 1997) is red-shifted compared with the unphotolyzed, initial state. In the subsequent step, this intermediate decays and a second species (named HR_{520} in the case of HR) appears that is blue-shifted with respect to its precursor. Finally, the rise and decay of a third, far-red-shifted intermediate (HR_{640} in the case of HR) completes the photocycle of both proteins. Interestingly, the rate-limiting step in the HR photocycle is the HR_{520} decay, whereas in BR-D85T the decay of the corresponding intermediate is much faster and thus not rate limiting. Here, the latter step is followed by the considerably slower decay of the late red-shifted intermediate, which is accompanied by the uptake of a chloride ion and progresses roughly at the same rate as the HR_{520} decay (several milliseconds). The photocycle steps involved in anion release into the cytoplasm are the decay of HR_{520} in HR and the decay of the second (blue-shifted) intermediate in BR-D85T. In an attempt to understand whether chloride pumping by HR and by BR-D85T is governed by the same underlying principles, we created BR-D85T double mutants with modifications in positions R175 and T178 and studied the resultant effects experimentally by employing chloride transport and binding assays as well as time-resolved optical absorbance spectroscopy.

MATERIALS AND METHODS

Mutagenesis and protein purification

The BR mutants D85T, D85T/R175Q, and D85T/T178V were constructed as described by Kunkel et al. (1987) and expressed homologously, except that the vector pEF191 (Ferrando et al., 1993) was replaced by the vector pUSMev (Schweiger et al., 1994). Colonies of halobacteria expressing the BR mutants displayed a characteristic green color distinguishing them from BR wild-type colonies, which were purple. The identities of the mutated proteins were determined by electrospray ionization mass spectroscopy (Hufnagel et al., 1996).

Isolation of BR from cells was carried out according to the standard procedure by Oesterhelt and Stoeckenius (1974). After lysis of the cells in the presence of DNAse I (Sigma, Steinheim, Germany), the resultant membrane fragments were washed with water and then purified by centrifugation on a sucrose gradient (25–45% w/w). Membrane fractions of buoyant density corresponding roughly to that of the purple membrane in wild-type BR (1.18 g/ml) were collected, washed repeatedly with water, and then resuspended in the appropriate buffer for spectroscopic measurements.

Chloride transport assays

The chloride-pumping activity of the BR mutants was determined in intact cells as described by Oesterhelt (1982). The cells were suspended in basal salt solution (4.3 M sodium chloride, 27 mM potassium chloride, 81 mM magnesium sulfate, pH 6) to give a total volume of 8 ml and an absorbance of 0.25 at 578 nm. The initial rate of light-induced chloride flux into the cells was monitored by recording the concomitant proton influx with a pH electrode in the presence of the protonophore carbonyl cyanide m-chlorophenylhydrazone (CCCP; 500 μM). Calibration of the electrode output was achieved by adding defined amounts of 0.1 N hydrochloric acid to the samples. All measurements were carried out in a thermostatted glass vessel at 25°C. A 100-W mercury lamp (HBO 100 W-2, Oriel, Stratford, CT) in combination with a heat protection filter (Calflex 3000, Balzers, Liechtenstein) and a yellow cutoff filter (OG-515, Schott, Mainz, Germany) served as a light source. The irradiance at the location of the sample was 40 mW/cm^2 and was reduced systematically by attenuating the light with neutral density filters (Oriel, Stratford, CT). Initial rates of chloride influx were determined at various light intensities and were extrapolated to light-saturating conditions with Lineweaver-Burk plots (double-reciprocal plot of initial rate versus irradiancy). The amount of BR in the assays was measured spectroscopically after purification (see above) using an extinction coefficient of 63,000 M^{-1} cm^{-1} at the absorbance maximum.

Chloride-binding assays

Chloride binding by the proteins was assayed spectroscopically by monitoring the chloride-induced blue-shift of their absorbance spectra. Samples (1 ml) containing ~10 μM protein in 1 M sodium sulfate (45 mM citrate, pH 5) were titrated with 3 M sodium chloride (45 mM citrate, pH 5) in a quartz cuvette up to chloride concentrations of 1.5–2 M. After each chloride addition, the spectrum of the sample was recorded with a lambda 2 (ultraviolet/visible) UV/VIS spectrometer (Perkin-Elmer, Norwalk, CT) and corrected for dilution.

Time-resolved absorbance spectroscopy

Transient absorbance difference spectra were recorded after flash excitation with a pulsed INDI Nd:YAG laser (λ = 532 nm, 2 mJ/pulse; Spectra-Physics, Mountain View, CA) after various delay times. Samples typically contained ~10 μM BR dispersed in mixtures of 3 M sodium chloride and 1 M sodium sulfate (both in 45 mM citrate, pH 5) to give specific chloride concentrations at constant ionic strength. For each mutant, data were recorded at five chloride concentrations between 0 and 3 M. Probe light from a xenon arc lamp (Oriel) was filtered by a heat protection filter (KG4, Schott), passed through the cuvette holding the sample, collected by a light guide, dispersed by a spectrograph, amplified by a gated lens-coupled intensifier (gate width $\leq$ 6 μs), and detected by a charge-coupled device

(CCD) camera (Princeton Applied Research, Princeton, NJ). For each data set, 40 transient difference spectra were taken at delay times that were evenly spaced on a logarithmic time scale between 10 μs and 100 ms. Each one of these spectra was generated by averaging the signals of 37 repeats. Some experiments required a higher time resolution (sub-microsecond range) in which case the gate width was shortened to 200 ns. The temperature of the samples was kept constant at 20°C.

RESULTS

Chloride transport

Chloride translocation rates under light-saturating conditions are a measure for the overall transport activity of the protein and are commonly expressed in number of chloride ions transferred per minute by one molecule of BR. At pH 6, all three mutants displayed comparable activities between 20 and 40 Cl^-/(min BR).

Chloride binding

Spectra from the chloride titration experiments were converted to difference spectra by referencing against the spectrum recorded in the absence of chloride (Fig. 1 *A*). For the purpose of noise reduction and simplification of curve fitting, each set of difference spectra was subjected to singular value decomposition (Hendler and Shrager, 1994) using the MATLAB software package (The MathWorks, Natick, MA). Because the effective rank of the data matrices was always equal to or smaller than two, the **U**-, **V**-, and **S**-matrices could be truncated after their first two columns. The two resultant **V**-vectors were then fit simultaneously to Eq. 1 *a* (Fig. 1 *C*):

$$\frac{[BR]}{[BR_t]} = \frac{1}{[Cl^-]/K_d + 1} \tag{1a}$$

with

$$K_d = \frac{[Cl^-][BR]}{[BR{\cdot}Cl^-]} \tag{1b}$$

and

$$[BR_t] = [BR] + [BR{\cdot}Cl^-] \tag{1c}$$

In Eq. 1, *a–c*, [BR] was the concentration of free protein, $[BR{\cdot}Cl^-]$ the concentration of chloride-bound protein, $[BR_t]$ the total protein concentration, $[Cl^-]$ the bulk chloride concentration, and K_d the dissociation constant. The obtained dissociation constants for BR-D85T and BR-D85T/R175Q were 221 and 205 mM, respectively and therefore identical within experimental error. In the case of D85T/T178V, the dissociation constant was considerably larger (1.7 M). The analysis also provided a difference spectrum describing the typical blue-shift that accompanied chloride binding (Fig. 1 *B*). The shape of this spectrum was identical for all three mutants and was dominated by a

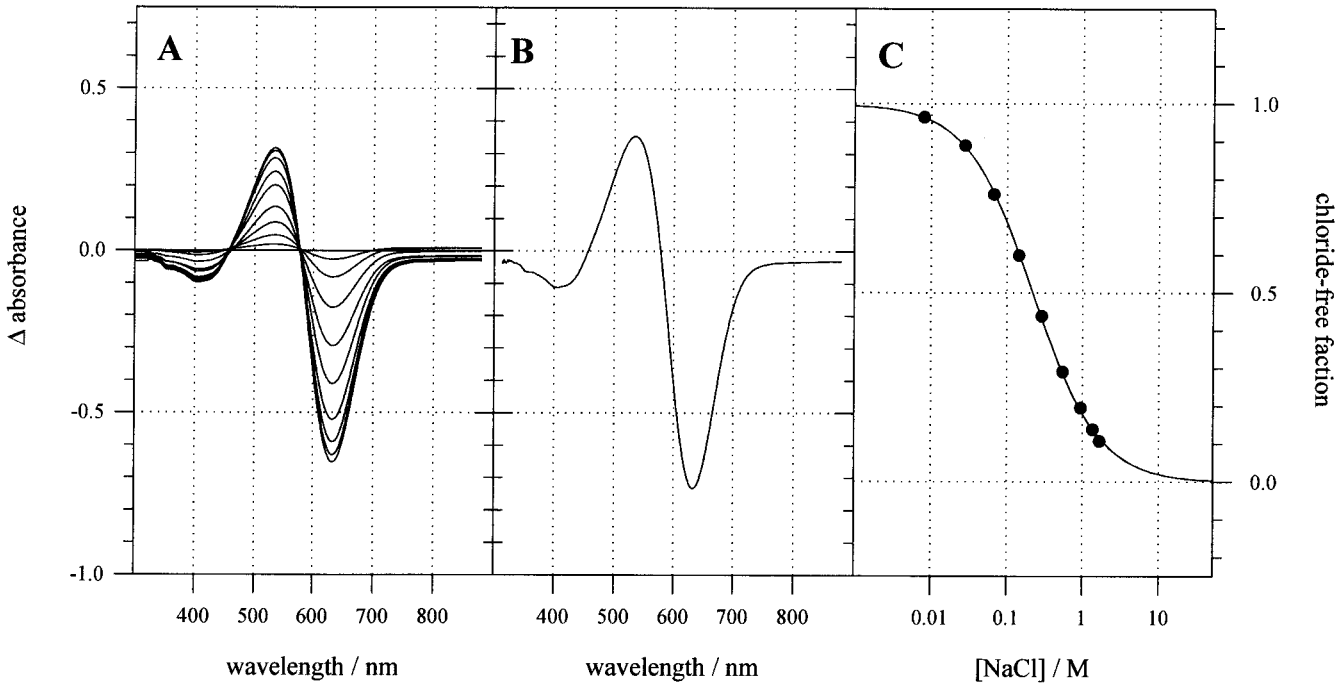

FIGURE 1 Titration of BR-D85T with sodium chloride (50 mM citrate, pH 5). (*A*) Difference spectra referenced against the spectrum taken in the absence of chloride. Increasing amplitudes indicate increasing chloride concentrations (0, 8, 28, 67, 143, 286, 543, 940, 1350, and 1660 mM). (*B*) Spectral amplitude describing the transition upon chloride binding as obtained from the fit. (*C*) First column of the V-matrix (●) and fit (——).

two-state transition accompanied by a small loss of absorbance around 410 nm with increasing chloride concentration. In the case of BR-D85T/T178V, the large K_d value was also reflected in the time-resolved flash photolysis data (see below), because the size of the laser-induced difference amplitudes displayed a chloride concentration dependence very similar to the one observed in the titration experiments.

Time-resolved absorbance spectroscopy

A typical set of transient absorbance spectra of BR-D85T recorded in the presence of 2.25 M chloride between 250 ns and 100 ms is shown in Fig. 2. The spectral development in this time range could be subdivided into three stages. Initially, a red-shifted intermediate (P_1) decayed with lifetimes in the sub-microsecond range to yield a species (P_2) that was slightly blue-shifted compared with the primary photoproduct (Fig. 2 *A*). The second phase took place between 10 μs and 1 ms and was dominated by the conversion of P_2 into a more red-shifted species (P_3, Fig. 2 *B*). In the third and final stage, intermediate P_3 returned to the initial state within a few milliseconds (Fig. 2 *C*).

In the presence of chloride, the photocycle of all three BR mutants displayed the same general features except for the actual values of the rate constants, which will be discussed below. Because the last two steps of the photocycle were of particular interest, most experiments were performed between 10 μs and 100 ms with increased time resolution.

Kinetic analysis started with singular value decomposition of the data matrix (Henry and Hofrichter, 1992). The first three columns of the **U**- and **V**-matrices with their corresponding singular values proved to be a sufficient representation of the original data matrix. Including additional columns only added noise to the data without changing the results of the further analysis. Between 10 μs and 100 ms, multi-exponential fitting using two apparent rate constants gave adequate fits to the data. Fig. 3 shows the two spectral amplitudes associated with the apparent rate constants for BR-D85T in 2.25 M sodium chloride.

The chloride dependence of the photocycle steps was explored by varying systematically the chloride concentration in the sample. No chloride dependence was detected for the rapid decay of the first intermediate, P_1 (data not shown), whereas the rate constants describing the decay of the second intermediate (k_2) displayed a slight chloride dependence for all three mutants (Fig. 4 *A*). In BR-D85T, k_2 increased with increasing chloride concentrations. The same behavior was observed for BR-D85T/R175Q, except that k_2 was somewhat smaller at all chloride concentrations. In contrast, BR-D85T/T178V displayed quite a different pattern: k_2 decreased with increasing chloride concentrations

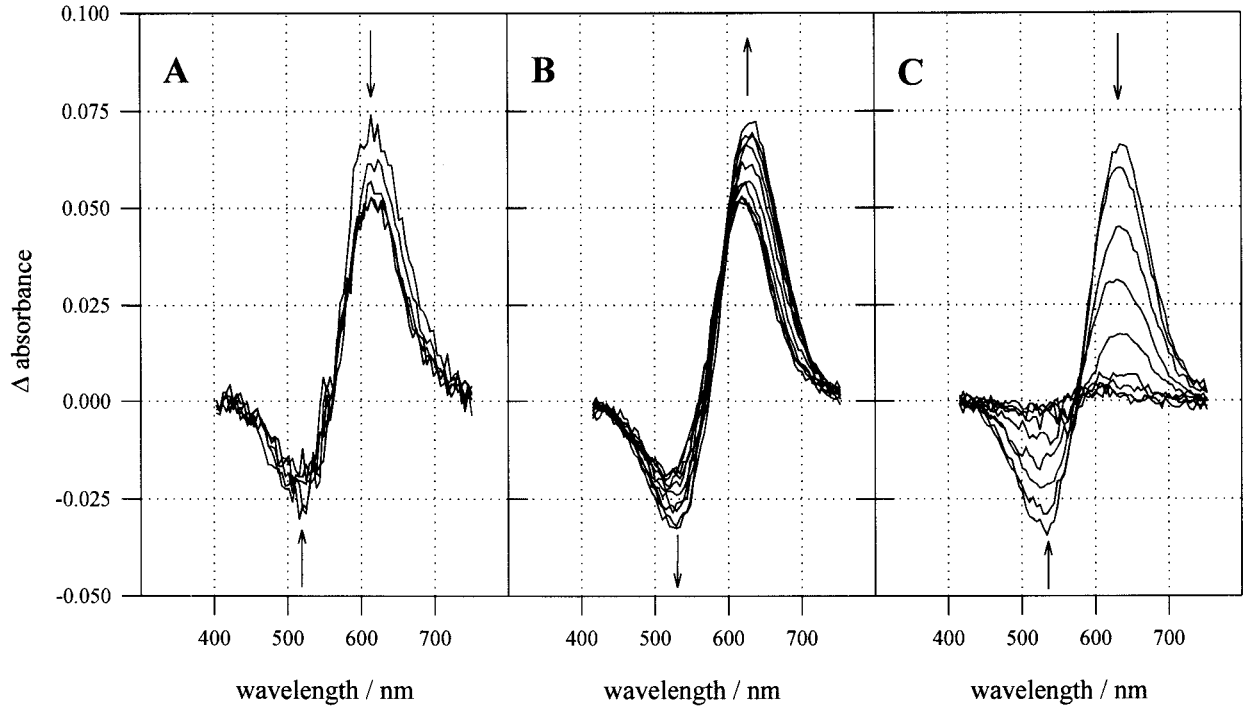

FIGURE 2 Transient absorbance difference spectra after excitation of BR-D85T (2.25 M NaCl, 0.25 Na_2SO_4, 45 mM citrate, pH 5) with a laser pulse at 532 nm (2 mJ/pulse). Arrows indicate spectral changes with increasing time. (*A*) First phase: decay of the initial photoproduct, P_1, and formation of P_2 (delays: 250 ns, 630 ns, 1.5 μs, 4 μs, and 10 μs). (*B*) Second phase: decay of P_2 and formation of P_3 (delays: 13, 20, 32, 50, 79, 130, 200, 320, 500, and 790 μs). (*C*) Third phase: decay of P_3 and recovery of the initial state (delays: 1.3, 2, 3.2, 5, 7.9, 13, 20, 32, and 50 ms).

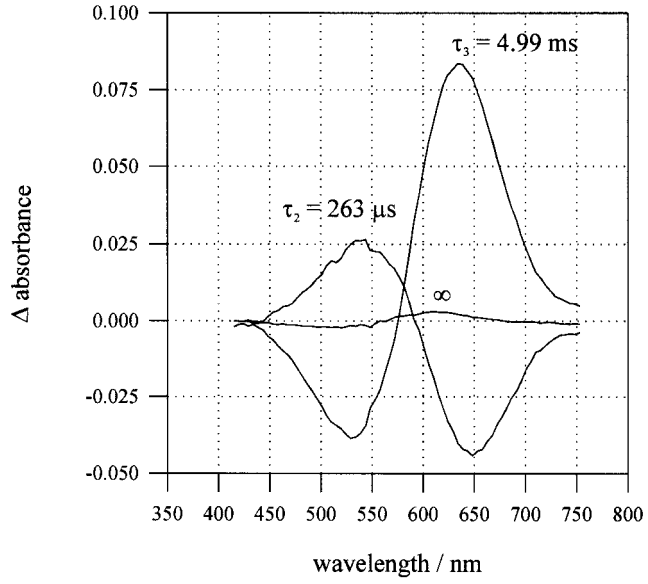

FIGURE 3 Results of singular value decomposition and multi-exponential fitting of a data set recorded between 10 μs and 50 ms. Spectral amplitudes are associated with the following apparent lifetimes: 263 μs and 4.99 ms. Sample: BR-D85T in 2.25 M NaCl, 0.25 M Na_2SO_4, and 45 mM citrate at pH 5.

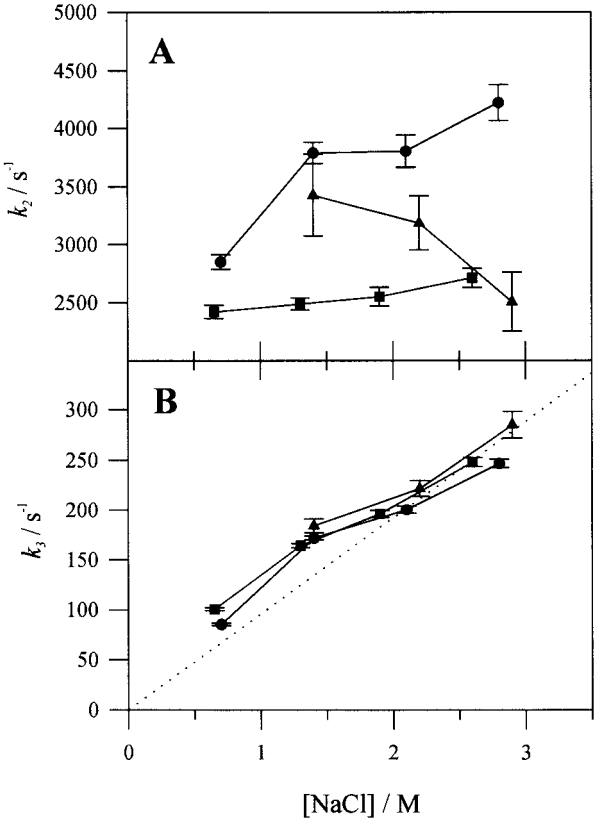

FIGURE 4 Dependence of rate constants k_2 and k_3 on chloride concentration (●, BR-D85T; ■, BR-D85T/R175Q; ▲, BR-D85T/T178V). The dotted line in *B* was obtained by linear regression for BR-D85T. Error bars indicate 95% confidence levels, which were calculated according to Nagle et al. (1982).

and at high chloride concentrations was actually smaller than in the case of the two other mutants.

Unlike k_2, the rate constant characterizing the last step in the photocycle, k_3, was virtually indistinguishable for the three mutants (Fig. 4 *B*). Furthermore, k_3 exhibited a pronounced chloride dependence. As shown in Fig. 4 *B*, this dependence was linear and could be described accurately by a straight line of positive slope passing through the origin of the graph (Fig. 4 *B*). This observation was consistent with earlier reports (Sasaki et al., 1995; Tittor et al., 1997) suggesting that this step in the photocycle was accompanied by the uptake of a chloride ion from the bulk. In this case, the measured apparent rate constants (k_{app}) were pseudo-first-order and their chloride dependence permitted the extraction of the true second-order rate constants, *k*, according to Eq. 2:

$$k_{app} = k[Cl^-] \quad (2)$$

As demonstrated for BR-D85T in Fig. 4 *B*, *k* could be obtained by linear regression and had the following values: 96 ± 7 L/(mol s) for BR-D85T, 104 ± 8 L/(mol s) for BR-D85T/R175Q, and 105 ± 8 L/(mol s) for BR-D85T/T178V.

In the absence of chloride, the spectral development was dominated by the rapid decay of an early red-shifted intermediate (data not shown). This decay could be modeled by one or two exponentials with congruent spectral amplitudes and lifetimes smaller than 10 μs. Because the photocycle in the absence of chloride was essentially completed in the early microsecond time range, data recorded between 10 μs and 100 ms in the presence of chloride did not contain notable spectral contributions from the chloride-free photocycle. Furthermore, the selected chloride concentrations were almost always distinctly larger than the respective chloride dissociation constant so that the majority of the BR molecules was actually bound to chloride (76% of BR-D85T at 0.7 M NaCl, for example) and therefore underwent the chloride-bound photocycle rather than the chloride-free one.

DISCUSSION

We have used site-directed mutagenesis in combination with transport assays, dissociation constant determinations, and time-resolved spectroscopy to explore the functions of residues R175 and T178 in the chloride-pumping BR-mutant D85T. First, we will briefly review and complement already existing evidence on the photocycle of BR-D85T because this type of data provides the most detailed information on the ion translocation process. Kinetic effects caused by mutating residues R175 and T178 will be taken

into account in order to propose potential functions of these residues. We will then inspect the recently published three-dimensional structures of BR and HR to test the feasibility of the assigned roles of R175 and T178 considering their positions in space. Finally, we will determine whether the postulated functions are compatible with the experimental results from the chloride binding and translocation studies.

Photocycle of BR-D85T and the kinetic effects of mutations R175Q and T178V

Despite slightly different experimental conditions (such as pH and nature of the transportable anion), the results presented in this study are in agreement with earlier reports on the photocycle kinetics of the single mutant BR-D85T. The triphasic spectral development has been recognized but not analyzed quantitatively by Sasaki et al. (1995), and the chloride dependence of the rate-limiting step has been described in detail by Tittor et al. (1997). In the simplest case, the photocycle of BR-D85T can be modeled adequately by an unbranched kinetic scheme as displayed in Fig. 5. No back reactions are assumed because the simplistic shapes of the fitted spectral amplitudes in Fig. 3 do not indicate the presence of more than two species at the same time. As the individual steps in the photocycle are sufficiently separated in time (the rate constants differ by factors between ten and several hundred), the apparent rate constants as obtained from the analysis described above are actually equal to the microscopic rate constants.

After photoisomerization (symbolized by I* in accordance with the IST model, see Introduction), the early difference spectra in the sub-microsecond range (Fig. 2 *A*) indicate the existence of a red-shifted intermediate, P_1, which closely resembles the K intermediate in wild-type BR or the HR_{600} intermediate in HR. As with similar observations made in HR from *Halobacterium salinarum* (Tittor et al., 1987; Váró et al., 1995c) and *Natronobacterium pharaonis* (Váró et al., 1995a,b), the subsequent blue-shift in the absolute absorbance spectrum that accompanies the rise of

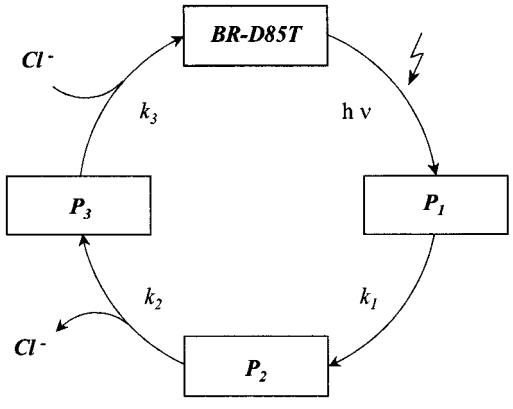

FIGURE 5 Proposed scheme for the photocycle of BR-D85T.

intermediate P_2 can be attributed to an altered charge distribution in the vicinity of the protonated Schiff base caused by the movement of the transported chloride ion, the Schiff base itself, or both (T). The only difference concerns the extent of the blue-shift that is more pronounced in HR than in BR-D85T. To attain vectorial ion transport, an accessibility switch (S) must follow the previous events. During the next step, the conversion of P_2 to P_3, the chloride ion is presumably released to the cytoplasm (T). Despite the lack of direct experimental evidence for this assumption, it appears reasonable for the following arguments. Chloride ion release from the vicinity of the Schiff base cannot occur in any step before the P_2-to-P_3 transition because this ion has not yet moved beyond the protonated Schiff base (see Ames et al., 1992, for a comparison with HR). Likewise, because the x-ray structure of HR does not show a chloride ion anywhere in the cytoplasmic part of the unphotolyzed state (Kolbe et al., 2000), the conjecture of early release of such a chloride ion near the cytoplasmic surface and its replacement by the chloride ion from the binding site later in the photocycle lacks support. The last step comprises reisomerization (I) and the second accessibility switch (S). It ultimately completes the cycle via thermal relaxation of the P_3 intermediate to the initial state and the uptake of a chloride ion from the bulk. Most likely, the chloride ion binds directly to the extracellular binding side. Alternatively, the rate-limiting step could comprise two events, such as a chloride-induced, slow accessibility change from the cytoplasmic to the extracellular side (causing the observed chloride dependence) that is followed instantaneously by fast chloride binding at the extracellular binding site. Unfortunately, the kinetic data of this study do not allow a distinction between these two scenarios. In terms of the IST model, the sequence I*TSTIS applies to both cases (Oesterhelt, 1998) because the anion re-uptake does not involve transfer directly to the Schiff base and is thus not considered a transfer process.

Replacing the cytoplasmic residues R175 and T178 affects only the transition from P_2 to P_3 whereas the last step in the photocycle remains unchanged. This observation is consistent with the presumption that the P_2-to-P_3 transition represents an event at the cytoplasmic side of the membrane, presumably anion release. It is also noteworthy that the changes upon mutation of the two residues are quite distinct. Substitution of R175 results essentially in an overall reduction of the rate constant k_2. Replacing T178, on the other hand, not only causes a decrease in k_2 but also changes the chloride dependence of the process. Unlike in BR-D85T and BR-D85T/R175Q, k_2 decreases with increasing chloride concentration. This points to the notion that T178 plays a fundamental role in the anion release event whereas the function of R175 is of secondary importance. It is plausible that the functions of the arginine/threonine pair are the same as those of the corresponding pair of residues in HR (R200 and T203) (Rüdiger and Oesterhelt, 1997). Because the

consequences of replacing T203 in HR were more significant than those of replacing R200, it was concluded that the former interacts directly with the transported anion in the cytoplasmic part of the channel whereas the latter influences anion release more indirectly, perhaps by control of the local protein structure. When comparing the two studies it is important to realize that the HR experiments were performed in saturated sodium chloride solutions whereas BR-D85T was measured at lower chloride concentrations (Fig. 4 *A*). Extrapolating the values for k_2 to 4.3 M chloride emphasizes even more the drastic changes due to the removal of T178.

As mentioned above, the rate constants of the rate-limiting step in the photocycle (k_3) are identical for all three mutants at any chloride concentration. The fact that k_3 is linearly dependent on bulk chloride concentration with a zero intercept (Fig. 4 *B*) implies that this step is accompanied by chloride ion uptake from the bulk phase, most likely at the extracellular binding site of the protein. Because both R175 and T178 are localized at the cytoplasmic side, they are not expected to be involved in this process, and therefore their mutation should not impair the kinetics of this step, which is exactly what was observed experimentally.

Structural considerations

Recently, the three-dimensional structures of BR and HR have become available (Pebay-Peyroula et al., 1997; Essen et al., 1998; Luecke et al., 1999a; Kolbe et al., 2000), offering the opportunity to assess the compatibility of the locations of residues R175 and T178 with their assumed functions. Fig. 6 offers a view from the cytoplasmic side on the positions of the R175/T178 pair in BR (Fig. 6 *A*) and the R200/T203 pair in HR (Fig. 6 *B*), respectively. In both proteins, the arginine points away from the center of the seven-helix assembly where the putative ion translocation pathway is located. This position is in obvious contrast to the alignment of the arginine from the extracellular arginine/threonine pair (R82/T85 in BR-D85T and R108/T111 in HR) whose orientation toward the interior of the protein is consistent with its observed function in anion binding. Although the structures represent the unphotolyzed state and do not provide any information about conformational changes that occur during the photocycle, the position of the arginine residue is so unfavorable that direct contact with the transported anion seems rather unlikely. Alternatively, the arginine could exert a long-range influence on the chloride ion mediated by electrostatic interactions that participate in a larger network of electrical charges. Most likely, however, the position of the arginine supports the idea that this residue does not have a specific transport function and that its mutation may cause a small local structural distortion that is capable of impairing the anion release slightly without affecting it in a fundamental way. Nevertheless, the arginine residue seems essential because a basic amino acid in this particular position is highly conserved not only in HR but also in BR and sensory rhodopsins of many halophiles (Ihara et al., 1999).

In contrast, the side chain of T178 points to the center of the BR molecule and might therefore interact directly via its hydroxyl group with the transported chloride ion once the latter enters the cytoplasmic part of the ion channel. Additional support for this notion arises from the close proximity of T178 to a conserved water molecule (both in BR and HR), which might help solvate the chloride ion as it reaches this region of the protein. The importance of water molecules in ion transport by transmembrane proteins has been recognized before (Papadopoulos et. al., 1990; Luecke et al., 1999b). A convincing illustration of this presumption is BR, in which proton transport stops entirely if the relative hu-

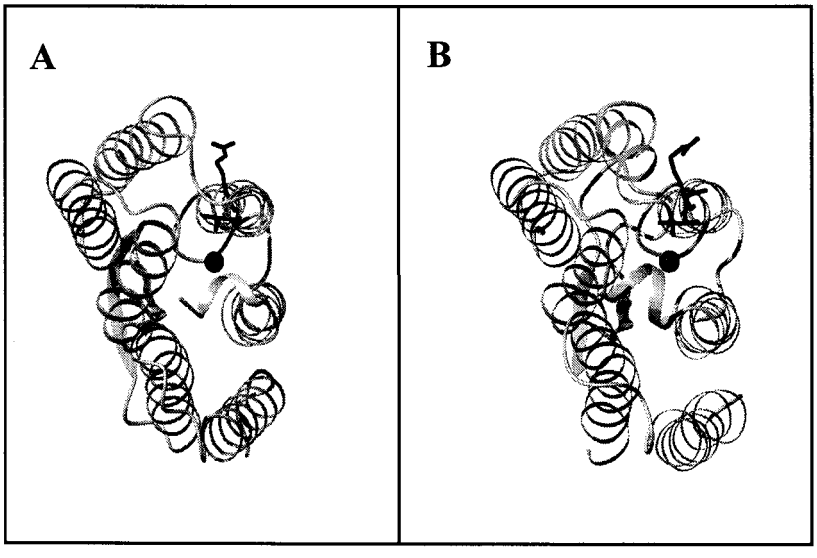

FIGURE 6 Positions of cytoplasmic residues R175 and T178 in BR (*A*) (Luecke et al., 1999a) and R200 and T203 in HR (*B*) (Kolbe et al., 2000). Residues are shown as black stick models, and the water molecule is represented by the black sphere. View from the cytoplasmic side of the membrane. The figure was prepared with the program MOLMOL (Koradi et al., 1996).

midity drops below 50% (Hauss et al., 1997). Overall, the three-dimensional structure is in agreement with the mutagenesis data because replacement of the threonine by valine has significant consequences for the anion release event at physiological chloride concentrations.

Chloride binding and transport

The dissociation constants (K_d) are a measure of the affinity of the protein in the unphotolyzed state for the chloride ion. The x-ray structure of HR has unambiguously located the chloride binding site (Kolbe et al., 2000) at the extracellular side of the protein. Taking into account the great structural similarities between HR and BR, the binding site of BR-D85T is most likely in the same place as in HR. Consequently, the R175/T178 pair and the binding site are well separated in space for which reason it was anticipated that mutating these residues should not, analogous to the situation in HR (Rüdiger et al., 1997), alter the value of K_d. This is true in the case of R175 whose substitution by glutamine does not change K_d. The increase in K_d as a result of the replacement of T178 by valine, however, is rather surprising. Certainly, direct interactions between the threonine and the chloride ion in the binding site cannot account for this phenomenon because they are too far apart. A possible explanation is the type of long-range interactions as they were observed in certain mutants of BR (Balashov et al., 1996; Alexiev et al., 2000). These interactions are believed to be mediated by salt bridges or hydrogen-bond networks and may be effective over ranges as far as the distance between the extra- and intracellular loops (Alexiev et al., 2000) or the extracellular surface and the Schiff base in BR (Balashov et al., 1996). In the absence of a three-dimensional structure, however, it remains difficult to verify the existence of these long-range effects in BR-D85T.

It should be emphasized that the increase in K_d in the case of BR-D85T/T178V does not necessarily warrant a decrease in k_3, the rate constant describing the decay of the last photocycle intermediate, P_3. Although both parameters characterize a reaction that involves the binding of a chloride ion resulting in the formation of BR in its unphotolyzed state, they potentially refer to different educts. Whereas K_d describes chloride binding to the chloride-free unphotolyzed state, k_3 characterizes chloride binding to a photocycle intermediate that is not necessarily identical to the chloride-free unphotolyzed species. For this reason, a direct comparison of the two constants is not straightforward.

The small negative peak around 420 nm in Fig. 1 *A* can be attributed to a partial protonation of the Schiff base. Apparently, the pK_a of the Schiff base is chloride dependent inasmuch as the presence of a negatively charged chloride ion in close proximity of the Schiff base favors protonation of the latter. This phenomenon has been described in detail elsewhere (Brown et al., 1996).

The overall chloride transport activity of the three mutants is essentially the same, which is consistent with the rest of the evidence. For the translocation activity to be the same, the extent of ion binding to BR has to be identical as the rate-limiting step progresses with the same velocity in all three cases. At first sight, this appears to be in contrast with the lower affinity of BR-D85T/T178V for chloride. However, it should be pointed out that the activity assays were conducted under chloride-saturating conditions with the chloride concentrations (4.3 M NaCl) clearly exceeding K_d, even in the case of BR-D85T/T178V ($K_d \approx 1.7$ M, 72% of protein bound to chloride). Consequently, a large majority of the BR molecules is bound to chloride, which, together with similar values for k_3, accounts for equal translocation activities.

Interestingly, the transport activities of all three mutants are ~10-fold lower than the activity of HR in intact cells (380 chloride ions/(min HR); Oesterhelt, 1982) despite the fact that all proteins require a few milliseconds to complete their photocycles and that affinities are such that chloride saturation occurs under the conditions of the assays. Although the exact reasons are unknown, there are several possible explanations for this observation. First, it has been shown that BR-D85T can operate in three different ion transportation modes, one chloride- and two proton-pumping modes (Tittor et al., 1997). It is possible that the proton translocation modes are active under the conditions of the transport assays, thereby reducing the fraction of BR molecules actually pumping chloride ions. Another possibility is a lag time between completion of the photocycle as monitored in the UV/VIS and the absorption of a second photon permitting reentry into the photocycle. Such delays could be caused by structural rearrangements required by the protein to get back to its initial state. If these rearrangements do not affect the chromophore, they escape detection by the spectroscopic experiments in the UV/VIS region. However, it should be noted that no such refractory periods were found in wild-type BR (Dancshazy et al., 1986). Overall, the low transport activities of the BR-D85T mutants appear somewhat surprising in the light of the kinetic and binding studies, but are not entirely unexpected if one realizes that even proteins optimized by evolution such as wild-type BR and HR display transport activities that are considerably lower than expected from the time they require to complete their photocycles.

CONCLUSIONS

Using site-directed mutagenesis, we have demonstrated that the functions of the cytoplasmic residues R175/T178 in BR-D85T during chloride release are comparable to those of R200/T203 in HR. Whereas the arginine is primarily of structural importance, the threonine is likely to make direct contact with the transported chloride ion. Although not proof, the presented findings are yet another argument in

favor of closely related anion translocation mechanisms in BR mutants and HR. This hypothesis was originally put forward after the discovery that a single point mutation could turn the proton pump BR into an anion pump with properties very similar to those of HR (Sasaki et al., 1995; Tittor et al., 1997). Additional support originated from spectroscopic studies (Brown et al., 1996), sequence analysis (Ihara et al., 1999), and structural studies both on HR (Havelka et al., 1995; Kolbe et al., 2000) and BR (Luecke et al., 1999a,b). Presumably, the overall protein structure provides the capabilities for both proton and chloride translocation, and only minor modifications determine the ion specificity and the direction of transport.

We are grateful to Bettina Brustmann for technical assistance in protein purification. We also thank Michael Kolbe for help regarding the preparation of Fig. 6.

This work was supported by the Deutsche Forschungsgemeinschaft (SFB 533).

REFERENCES

Alexiev, U., R. Mollaaghababa, H. G. Khorana, and M. P. Heyn. 2000. Evidence for long range allosteric interaction between the extracellular and cytoplasmic parts of bacteriorhodopsin from the mutant R82A and its second site revertant R82A/G231C. *J. Biol. Chem.* 275:13431–13440.

Ames, J. B., J. Raap, J. Lugtenburg, and R. A. Mathies. 1992. Resonance Raman study of halorhodopsin photocycle kinetics, chromophore structure, and chloride-pumping mechanism. *Biochemistry.* 31:12546–12554.

Balashov, S. P., E. S. Imasheva, R. Govindjee, and T. G. Ebrey. 1996. Evidence that aspartate 85 has a higher pK_a in all-*trans* than in 13-*cis* bacteriorhodopsin. *Biophys. J.* 70:473–481.

Brown, L. S., R. Needleman, and J. K. Lanyi. 1996. Interaction of proton and chloride transfer pathways in recombinant bacteriorhodopsin with chloride transport activity: implications for the chloride translocation mechanism. *Biochemistry.* 35:16048–16054.

Dancshazy, Z., G. I. Groma, D. Oesterhelt, and J. Tittor. 1986. The photochemical cycle of bacteriorhodopsin has no refractory period. *FEBS Lett.* 196:198–202.

Dioumaev, A. K., and M. S. Braiman. 1997. Nano- and microsecond time-resolved FTIR spectroscopy of the halorhodopsin photocycle. *Photochem. Photobiol.* 66:755–763.

Essen, L.-O., R. Siegert, W. D. Lehmann, and D. Oesterhelt. 1998. Lipid patches in membrane protein oligomers: crystal structure of the bacteriorhodopsin-lipid complex. *Proc. Natl. Acad. Sci. U.S.A.* 95: 11673–11678.

Ferrando, E., U. Schweiger, and D. Oesterhelt. 1993. Homologous bacterioopsin-encoding gene expression via site-specific vector integration. *Gene.* 125:41–47.

Haupts, U., J. Tittor, E. Bamberg, and D. Oesterhelt. 1997. General concept for ion translocation by halobacterial retinal proteins: the isomerization/switch/transfer (IST) model. *Biochemistry.* 36:2–7.

Hauss, T., G. Papadopoulos, S. A. W. Verclas, G. Büldt, and N. A. Dencher. 1997. Essential water molecules in the light-driven proton pump bacteriorhodopsin. *Physica B.* 234:217–219.

Havelka, W. A., R. Henderson, and D. Oesterhelt. 1995. Three-dimensional structure of halorhodopsin at 7 Å resolution. *J. Mol. Biol.* 247:726–738.

Hendler, R. W., and R. I. Shrager. 1994. Deconvolutions based on singular value decomposition and the pseudoinverse: a guide for beginners. *J. Biochem. Biophys. Methods.* 28:1–33.

Henry, E. R., and J. Hofrichter. 1992. Singular value decomposition: application to analysis of experimental data. *Methods Enzymol.* 210: 129–193.

Hufnagel, P., U. Schweiger, C. Eckerskorn, and D. Oesterhelt. 1996. Electrospray ionization mass spectroscopy of genetically and chemically modified bacteriorhodopsins. *Anal. Biochem.* 243:46–54.

Ihara, K., T. Umemura, I. Katagiri, T. Kitajima-Ihara, Y. Sugiyama, Y. Kimura, and Y. Mukohata. 1999. Evolution of the archaeal rhodopsins: evolution rate changes by gene duplication and functional differentiation. *J. Mol. Biol.* 285:163–174.

Kalaidzidis, IV, Y. L. Kalaidzidis, and A. D. Kaulen. 1998. Flash-induced voltage changes in halorhodopsin from *Natronobacterium pharaonis. FEBS Lett.* 427:59–63.

Kalaidzidis, IV, and A. D. Kaulen. 1997. Cl^--dependent photovoltage responses of bacteriorhodopsin: comparison of the D85T and D85S mutants and wild-type acid purple form. *FEBS Lett.* 418:239–242.

Kolbe, M., H. Besir, L.-O. Essen, and D. Oesterhelt. 2000. Structure of the light-driven chloride pump halorhodopsin at 1.8 Å resolution. *Science.* 288:1390–1396.

Koradi, R., M. Billeter, and K. Wüthrich. 1996. MOLMOL: a program for display and analysis of macromolecular structures. *J. Mol. Graph.* 14: 51–55.

Kunkel, T., J. D. Roberts, and R. A. Zakour. 1987. Rapid and sufficient site-specific mutagenesis without phenotypic selection. *Methods Enzymol.* 154:367–382.

Lanyi, J. K. 1990. Halorhodopsin, a light-driven electrogenic chloride transport system. *Physiol. Rev.* 70:319–330.

Ludmann, K., G. I. Ibron, J. K. Lanyi, and G. Váró. 2000. Charge motions during the photcycle of *pharaonis* halorhodopsin. *Biophys. J.* 78: 959–966.

Luecke, H., B. Schobert, H.-T. Richter, J.-P. Cartailler, and J. K. Lanyi. 1999a. Structure of bacteriorhodopsin at 1.55 Å resolution. *J. Mol. Biol.* 291:899–911.

Luecke, H., B. Schobert, H.-T. Richter, J.-P. Cartailler, and J. K. Lanyi. 1999b. Structural changes in bacteriorhodopsin during ion transport at 2 Å resolution. *Science.* 286:255–260.

Nagle, J. F., L. A. Parodi, and R. H. Lozier. 1982. Procedure for testing kinetic models of the photocycle of bacteriorhodopsin. *Biophys. J.* 38:161–174.

Oesterhelt, D. 1982. Reconstitution of the retinal proteins bacteriorhodopsin and halorhodopsin. *Methods Enzymol.* 88:10–17.

Oesterhelt, D. 1995. Structure and function of halorhodopsin. *Isr. J. Chem.* 35:475–494.

Oesterhelt, D. 1998. The structure and mechanism of the family of retinal proteins from halophilic archaea. *Curr. Opin. Struct. Biol.* 8:489–500.

Oesterhelt, D., and W. Stoeckenius. 1974. Isolation of the cell membrane of *Halobacterium halobium* and its fractionation into red and purple membrane. *Methods Enzymol.* 31:667–678.

Papadopoulos, G., N. A. Dencher, G. Zaccai, and G. Büldt. 1990. Water molecules and exchangeable hydrogen ions at the active centre of bacteriorhodopsin localized by neutron diffraction: elements of the proton pathway? *J. Mol. Biol.* 214:15–19.

Pebay-Peyroula, E., G. Rummel, J. P. Rosenbusch, and E. M. Landau. 1997. X-ray structure of bacteriorhodopsin at 2.5 angstroms from microcrystals grown in lipidic cubic phases. *Science.* 277:1676–1681.

Rüdiger, M., U. Haupts, K. Gerwert, and D. Oesterhelt. 1995. Chemical reconstitution of a chloride pump inactivated by a single point mutation. *EMBO J.* 14:1599–1606.

Rüdiger, M., and D. Oesterhelt. 1997. Specific arginine and threonine residues control anion binding and transport in the light-driven chloride pump halorhodopsin. *EMBO J.* 16:3813–3821.

Sasaki, J., L. S. Brown, Y. S. Chon, H. Kandori, A. Maeda, R. Needleman, and J. Lanyi. 1995. Conversion of bacteriorhodopsin into a chloride ion pump. *Science.* 269:73–75.

Schweiger, U., J. Tittor, and D. Oesterhelt. 1994. Bacteriorhodopsin can function without a covalent linkage between retinal and protein. *Biochemistry.* 33:535–541.

Tittor, J., U. Haupts, C. Haupts, D. Oesterhelt, A. Becker, and E. Bamberg. 1997. Chloride and proton transport in bacteriorhodopsin mutant D85T: different modes of ion translocation in a retinal protein. *J. Mol. Biol.* 271:405–416.

Tittor, J., D. Oesterhelt, R. Maurer, H. Desel, and R. Uhl. 1987. The photochemical cycle of halorhodopsin: absolute spectra of intermediates obtained by flash photolysis and fast difference spectra measurement. *Biophys. J.* 52:999–1006.

Tittor, J., U. Schweiger, D. Oesterhelt, and E. Bamberg. 1994. Inversion of proton translocation in bacteriorhodopsin mutants D85N, D85T, and D85,96N. *Biophys. J.* 67:1682–1690.

Váró, G., L. S. Brown, J. Sasaki, H. Kandori, A. Maeda, R. Needleman, and J. K. Lanyi. 1995a. Light-driven chloride ion transport by halorhodopsin from *Natronobacterium pharaonis*. I. The photochemical cycle. *Biochemistry.* 34:14490–14499.

Váró, G., R. Needleman, and J. K. Lanyi. 1995b. Light-driven chloride ion transport by halorhodopsin from *Natronobacterium pharaonis*. II. Chloride release and uptake, protein conformation change, and thermodynamics. *Biochemistry.* 34:14500–14507.

Váró, G., L. Zimányi, X. Fan, L. Sun, R. Needleman, and J. K. Lanyi. 1995c. Photocycle of halorhodopsin from *Halobacterium salinarium*. *Biophys. J.* 68:2062–2072.

Zimányi, L., and J. K. Lanyi. 1989a. Low-temperature photoreactions of halorhodopsin. II. Description of the photocycle and its intermediates. *Biochemistry.* 28:1662–1666.

Zimányi, L., and J. K. Lanyi. 1989b. Transient spectroscopy of bacterial rhodopsins with an optical multichannel analyzer. II. Effects of anions on the halorhodopsin photocycle. *Biochemistry.* 28:5172–5178.

Zimányi, L., P. Ormos, and J. K. Lanyi. 1989. Low-temperature photoreactions of halorhodopsin. I. Detection of conformation substates of the chromoprotein. *Biochemistry.* 28:1656–1661.